Nanotechnology 23 (2012) 205503 (5pp) doi:10.1088/0957-4484/23/20/205503

Subnanometric stabilization of plasmon-enhanced optical microscopy

Taka-aki Yano[1,2,4], **Taro Ichimura**[1,2,5], **Shota Kuwahara**[1,6], **Prabhat Verma**[1,2] and **Satoshi Kawata**[1,2,3]

[1] Department of Applied Physics, Osaka University, Suita, Osaka 565-0871, Japan
[2] CREST, Japan Science and Technology Agency, Kawaguchi, Saitama 332-0012, Japan
[3] Nanophotonics Laboratory, RIKEN, The Institute of Physical and Chemical Research, 2-1 Hirosawa, Wako, Saitama 351-0198, Japan

E-mail: yano@ap.eng.osaka-u.ac.jp

Received 15 February 2012, in final form 3 April 2012
Published 30 April 2012
Online at stacks.iop.org/Nano/23/205503

Abstract

We have demonstrated subnanometric stabilization of tip-enhanced optical microscopy under ambient condition. Time-dependent thermal drift of a plasmonic metallic tip was optically sensed at subnanometer scale, and was compensated in real-time. In addition, mechanically induced displacement of the tip, which usually occurs when the amount of tip-applied force varies, was also compensated *in situ*. The stabilization of tip-enhanced optical microscopy enables us to perform long-time and robust measurement without any degradation of optical signal, resulting in true nanometric optical imaging with high reproducibility and high precision. The technique presented is applicable for AFM-based nanoindentation with subnanometric precision.

(Some figures may appear in colour only in the online journal)

1. Introduction

Tip-enhanced optical microscopy has been attracting much attention because of super-spatial resolution far beyond the diffraction limit of the probing light, along with an enhanced scattering efficiency [1]. This is due to a nanometallic tip, which plasmonically confines and enhances the probing light in the close vicinity of the tip apex. It becomes more powerful in terms of analytical power when it is combined with Raman spectroscopy, which is called tip-enhanced Raman scattering (TERS) spectroscopy. TERS has so far been applied to nano-analysis of various materials such as carbon nanomaterials [2–4], biomaterials [5–8] and semiconductors [9–11].

Similar to many other scanning probe microscopes (SPM), TERS microscopy also suffers from thermal drift due to the contraction or expansion of the system under ambient conditions. This results in an unwanted change in the relative position of the probe tip and the sample, degrading the image quality. If the behavior of this drift is known in a topographic measurement such as in atomic force microscopy (AFM), it is possible to compensate this drift by a post-measurement treatment of the data, because the drift of the system usually results only in a shift of the data points. However, since TERS microscopy is based on optical measurement, this method is no longer suitable for TERS. A drift during TERS measurement does not only mean a change in the relative position of tip and sample, but it also means a change in the relative position of the focal spot and tip. Since the light intensity within a focal spot usually has Gaussian variation, even a slight change in the tip position with respect to the focal spot would affect the optical process, such as the intensity of the Raman signal, which cannot be compensated after the measurement is completed. A typical drift of tip in an AFM-based system under ambient conditions is about 1–10 nm min^{-1}, which is enough to move the tip away from the center of a tightly focused laser spot during the measurement, as shown in figure 1(a). This results in the degradation of the plasmonically enhanced near-field optical signal, which is impossible to recover after the compilation

[4] Present address: Department of Electronic Chemistry, Tokyo Institute of Technology, 226-8502, Japan.

[5] Present address: Quantitative Biology Center, RIKEN, 565-0874, Japan.

[6] Present address: Department of Applied Chemistry, Chuo University, 112-8511, Japan.

 © 2012 IOP Publishing Ltd Printed in the UK & the USA

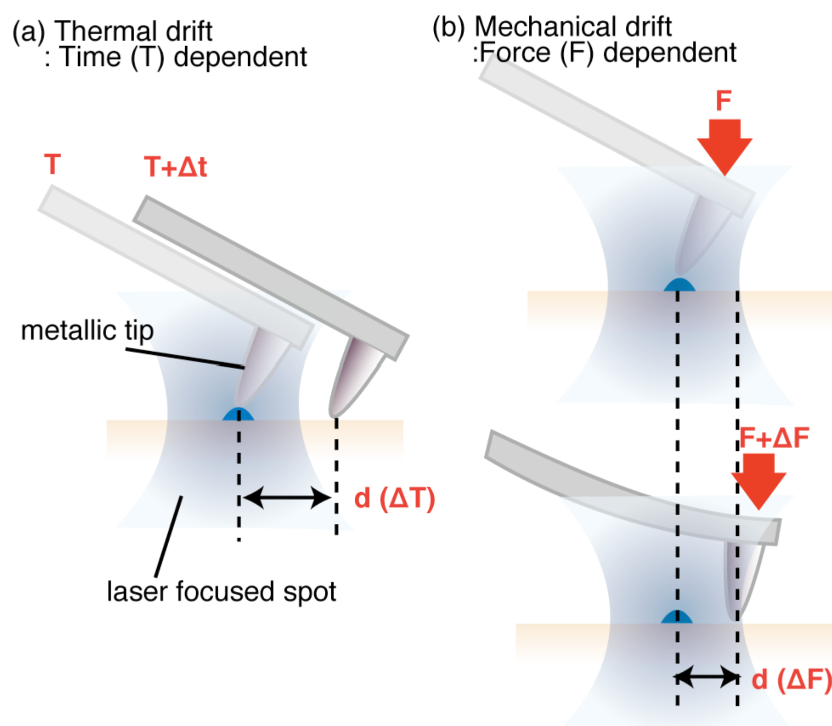

Figure 1. Schematics of (a) the time-dependent thermal drift and (b) the force-dependent mechanical drift of a metallic tip. Both of the drifts degrade precision and optical sensitivity.

of the measurement. The drift in the TERS system is a major obstacle in performing two-dimensional TERS imaging of a reasonable-sized sample, which requires several tens of minutes to complete the measurement. Therefore, it is necessary to have a method that can *in situ* compensate the drift, so that the tip stays stationary with respect to the laser spot during the entire measurement period. Further, we have recently developed an improved ultrahigh resolution TERS microscopy known as tip-pressurized TERS microscopy, where extremely high spatial resolution is achieved by locally pressurizing the sample by the apex of the probe tip [12, 13]. In this technique, the tip-applied force is intentionally changed during the TERS measurement, which bends the cantilever and results in mechanically induced lateral displacement of the tip in the direction of the long axis of the cantilever, as shown in figure 1(b). Since the mechanically induced drift varies with tip-applied force and results in a change of the relative position between tip and the focal spot, we again need a compensation method that works *in situ* during the measurement. Here in this paper, we demonstrate an optical technique for real-time and *in situ* compensation of thermal and mechanical drifts in TERS microscopy, which is robust against long-time measurements. This enables us to perform both the normal TERS and the tip-pressurized TERS optical imaging with a measurement precision of subnanometer scale.

2. Experimental details

A number of effective techniques for compensating the drift in SPMs under ambient conditions have been demonstrated so far, which have shown excellent results for topographic imaging. Estimation of the drift from cross-correlation between successively measured topographic images enabled us to track a single molecule on a surface [14, 15]. The atom-tracking method [16] using a circular motion of the tip over an individual molecule or atom provided effective drift compensation, and was applied to force spectroscopy of a single atom in ultrahigh vacuum [17]. The Kalman filter technique effectively estimated and predicted the drift in a short period of time by computing the standard means and the covariance [18]. The optical techniques provided a strong advantage in the real-time process of drift compensation [19–21]. With the use of external illumination of light, displacement of the SPM tip was interferometrically measured and compensated on a nanometer scale [19, 20]. The scattering method, which is often utilized for position sensing in optical trapping [22], was successfully applied to compensate the drift of both the AFM tip and the sample stage independently on an atomic scale in ambient conditions [21].

In order to meet the rising demand on stabilization of TERS microscopy, we developed a system for *in situ* and in real-time compensation of the drift of a plasmonic probe tip used in TERS microscopy, which is based on optical techniques [21]. Figure 2 shows a schematic of the system. This system is based on a conventional AFM-based TERS set-up, which is combined with a quadrant photodiode (QPD) for sensing the position of the tip. The AFM head and the sample stage are equipped with the inverted optical microscope, and are surrounded together by an acoustic enclosure. The enclosure enables not only prevention from external acoustic noise but also a temperature stability

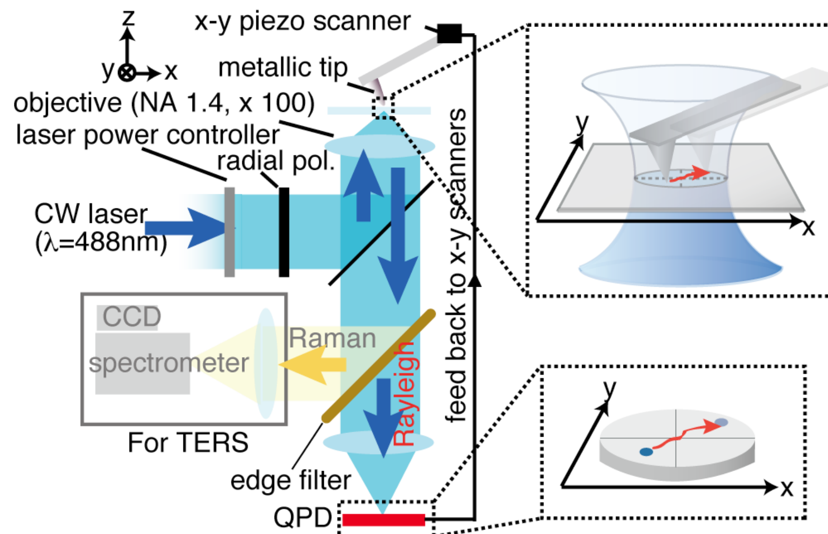

Figure 2. Optical system for the real-time drift sensing and compensation, which is equipped with an AFM-based TERS microscope.

of ±0.1 °C near the AFM head whereas the temperature fluctuates more than ±1 °C without the enclosure. Laser light with a wavelength of 488 nm is tightly focused using a high NA objective onto the metal-coated cantilever tip placed on the glass substrate. Rayleigh and Raman scattering from the tip apex are collected by the same objective, and are divided into two paths by the edge filter. The Rayleigh scattering signal is focused onto the center of the QPD detector, which corresponds to the tip positioned in the center of the focus spot. Displacement of the tip with respect to the center of the focus spot on the glass substrate is sensed by the difference signals of the QPD, i.e. the normalized difference signals from the left and right halves of the QPD for sensing displacement in the x direction, and from the top and bottom halves of the QPD for sensing displacement in the y direction. The displacements in the x and y directions are fed to piezoscanners of the x and y directions, respectively, under proportional–integral (PI) gain control. Incident laser power is stabilized by the laser intensity controller (BEOC, LPC-VIS) and is set to a few hundred μW, the value of which is usually utilized in TERS measurement. Incident polarization of the laser light is set to the radial polarization that is generated by a spirally varying retarder which consists of eight divided half-waveplates with a different direction of each slow axis. The tightly focused laser light with the radial polarization generates the dominant longitudinal field parallel to the tip axis, which provides a much stronger plasmonically enhanced field at the tip apex than that with the linear polarization. This enables us to detect the Rayleigh scattering from the tip apex with high signal-to-noise ratio. In addition to the enhancement of Rayleigh scattering, the radial polarization contributes to improving the sensitivity of position sensing. The radially polarized light generates a single intense spot of the longitudinal field in the center of the focus spot. On the other hand, the linearly polarized light generates two divided weak spots elongated perpendicular to the polarization direction, which gives anisotropic sensitivity in sensing the lateral displacement. That is why the radial polarization gives higher stabilized displacement sensitivity compared to the linear polarization.

3. Results and discussion

Using the position sensing system, compensation of time-dependent thermal drift was demonstrated in real time. As shown in figure 3(a), there are two major scattering components from the apex of the silver-coated Si cantilever tip in the tightly focused laser spot. One is plasmonically enhanced Rayleigh scattering from the silver surface, which is used for drift compensation. The other is plasmonically enhanced Raman scattering from the bare material (Si) of the tip, which is used to study the influence of the drift on optical stability of the plasmonically enhanced field at the tip apex. The dotted lines in figure 3(b) show the time-dependent lateral displacement (x and y directions) of the tip measured through the time-dependent change of the Rayleigh scattering. The tip consistently drifted in both x and y directions, and exhibited a lateral drift of ∼0.5 nm min^{-1} and ∼2.5 nm min^{-1}, respectively. Here, let us also note that, when the TERS system was not surrounded by an acoustic enclosure, the amount of lateral drift was more than three times larger. However, as shown by the solid lines in figure 3(b), when the time-dependent lateral displacement of the tip was compensated in real time with the use of the feedback control, the displacement was drastically reduced. The standard deviation of the displacement during drift compensation is estimated to be 0.7 nm in both x and y directions (see the inset in figure 3(b)), which realized subnanometric control over the drift of the tip in the center of the focus spot. In addition, during measurement and compensation of the thermal drift, plasmonically enhanced Raman scattering from the Si tip coated with silver was detected using the TERS system. Figure 3(c) shows Raman scattering from the Si tip, which was measured while monitoring the lateral drift of the tip for 40 min. Without real-time compensation of the lateral drift, Raman intensity gradually decreased as time passed, as

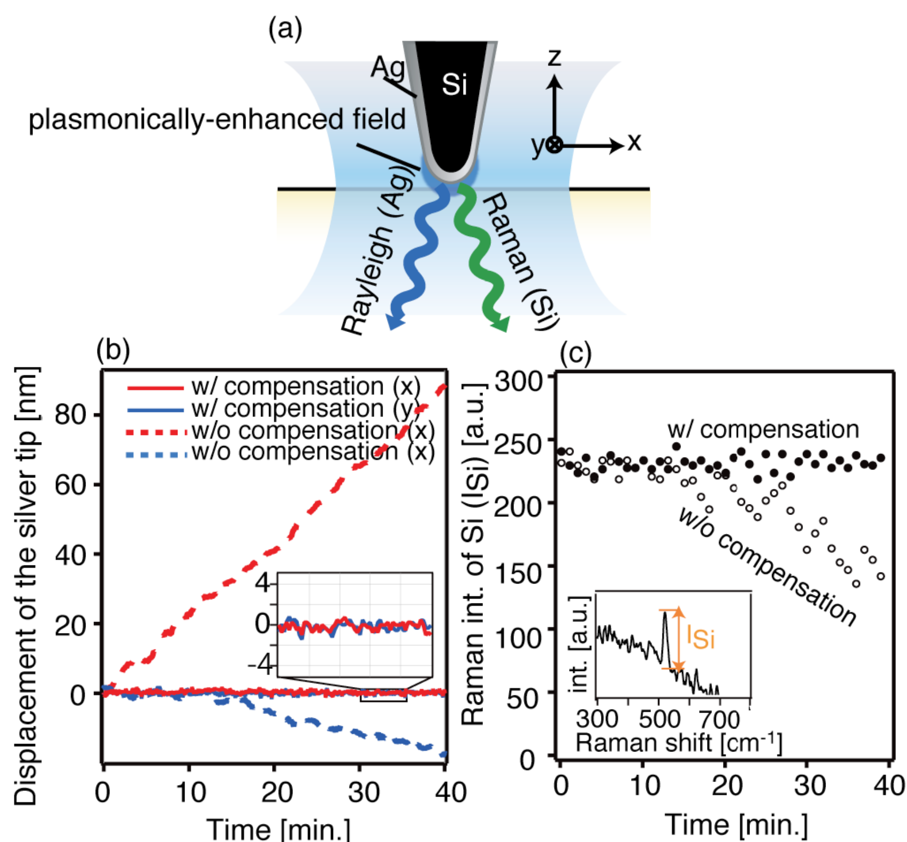

Figure 3. (a) Schematic of the scattering signals (Rayleigh and Raman) from a Si tip coated with silver, (b) time-dependent lateral displacement of the tip with (solid lines) and without (dotted lines) the scheme of drift compensation and (c) time-dependent change of Raman intensity with and without the compensation scheme. The inset shows a Raman spectrum from the silver-coated Si tip.

shown by the hollow data points in figure 3(c), following the time-dependent drift in figure 3(b). In 40 min, the Raman intensity went down by 40%, confirming that the tip was getting away from the center of the focus spot, and was losing the plasmonically enhanced field at the tip apex. This tendency degrades long-time TERS imaging, which usually needs the measurements to run for more than 1 h. On the other hand, when the drift was being compensated in real time, Raman intensity remained constant as shown by the solid data points in figure 3(c), revealing that the tip position was maintained in the exact center of the focus spot. This condition enables us to perform robust TERS imaging without any degradation of optical contrast.

In addition to the thermal drift, the mechanical drift of the tip is also a critical factor to degrade the precision of TERS experiments. When the base of the AFM cantilever moves down during a tip-pressurized TERS measurement in order to increase tip-applied force, the tip usually slides forward in the direction of the cantilever's long axis (i.e. the x axis in the inset of figure 4(a)) because of the tilt of the cantilever with respect to the sample (substrate) surface. In general, the force-induced drift is characterized simply by the cantilever's physical properties such as the length of the cantilever's long axis, the tilt angle and the spring constant. Cannara *et al* established a simple calculation method to predict the amount of the drift under a certain tip-applied force with an accuracy of within 15% [23]. Here we applied the above-described experimental technique to *in situ* compensation of the force-dependent drift with subnanometric precision. Figure 4(a) shows the lateral displacement of the tip measured while the tip-applied force was intentionally increased from 0.1 to 3 nN. The tip slid in the x direction with the coefficient of approximately 3.3 nm nN^{-1} whereas there was almost no displacement of the tip in the y direction. The experimentally measured drift in the x direction deviates by around 25% from the prediction (the dotted line in figure 4(a)) calculated with our cantilever's physical properties (spring constant: 0.1 N m^{-1}, cantilever length: 225 μm, tilt angle: 15°). This is because the spring constant of the cantilever usually varies from tip to tip. Figure 4(b) shows the lateral displacement compensated *in situ* while increasing the tip-applied force up to 3 nN. At every increment of 0.2 nN, which is expected to induce a drift of ∼0.6 nm in the x direction, the drift was compensated. Therefore, the tip remained at the same position with subnanometric accuracy when the tip-applied force varied. The technique of the drift compensation is also useful to improve the accuracy and precision of nanoindentation experiments using AFM as well as tip-pressurized near-field Raman experiments.

Finally, it is worth noting that, even though small-sized samples such as carbon nanotubes and DNA nanocrystals with sizes smaller than 10 nm were positioned under the silver tip, they did not affect the sensitivity and the accuracy of our drift compensation method. This is because scattering efficiency of

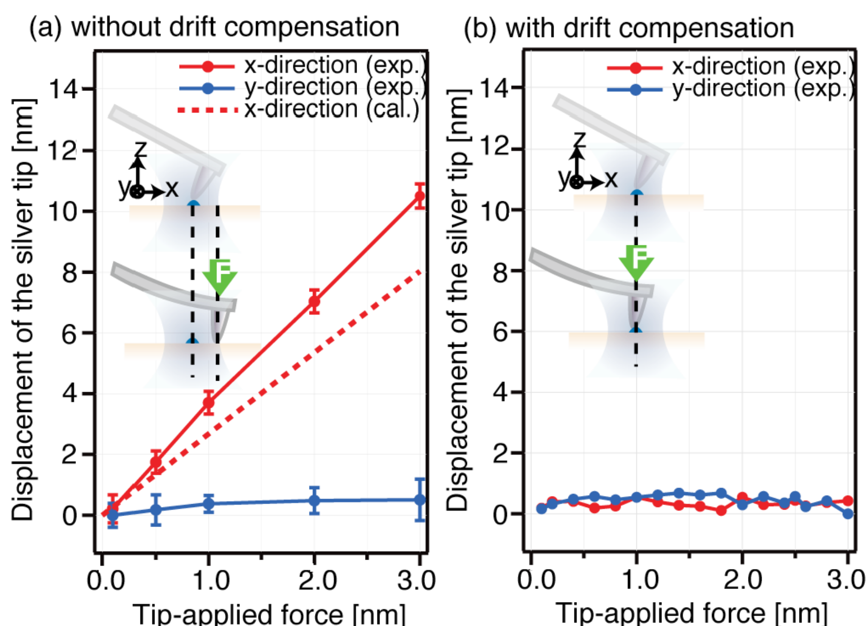

Figure 4. Force-dependent lateral displacement of the tip measured while increasing tip-applied force up to 3 nN (a) without and (b) with the compensation scheme.

these samples is much smaller than the metallic tip with the apex size of 40 nm. The influence of an additional scatterer with relatively large size on position sensing by QPD has been well studied in the optical trapping research [24].

Acknowledgments

The authors thank T Takarada for his preliminary experiments and F Futamatsu for discussion. This work was financially supported by the CREST (Core Research for Evolutional Science and Technology) project of JST (Japan Science and Technology Corporation). TY partially acknowledges financial support by a Grant-in-Aid for Young Scientists (B) no. 23760051 from the Ministry of Education, Culture, Sports, Science and Technology.

References

[1] Kawata S, Inouye Y and Verma P 2009 *Nature Photon.* **3** 388
[2] Hayazawa N, Yano T, Watanabe H, Inouye Y and Kawata S 2003 *Chem. Phys. Lett.* **376** 174
[3] Hartschuh A, Sánchez E J, Xie X S and Novotny L 2003 *Phys. Rev. Lett.* **90** 095503
[4] Saito Y, Verma P, Masui K, Inouye Y and Kawata S 2009 *J. Raman Spectrosc.* **40** 1434
[5] Ichimura T, Hayazawa N, Hashimoto M, Inouye Y and Kawata S 2004 *Phys. Rev. Lett.* **92** 220801
[6] Domke K F, Zhang D and Pettinger B 2007 *J. Am. Chem. Soc.* **129** 6708
[7] Bailo E and Deckert V 2008 *Angew. Chem. Int. Edn* **47** 1658
[8] Yeo B S, Mädler S, Schmid T, Zhang W and Zenobi R 2008 *J. Phys. Chem.* C **112** 4867
[9] Hayazawa N, Motohashi M, Saito Y, Ishitobi H, Ono A, Ichimura T, Verma P and Kawata S 2007 *J. Raman Spectrosc.* **38** 684
[10] Berweger S, Neacsu C C, Mao Y, Zhou H, Wong S S and Raschke M B 2009 *Nature Nanotechnol.* **4** 496
[11] Zhang D, Heinemeyer U, Stanciu C, Sackrow M, Braun K, Hennemann L E, Wang X, Scholz R, Schreiber F and Meixner A J 2010 *Phys. Rev. Lett.* **104** 056601
[12] Yano T, Verma P, Saito Y, Ichimura T and Kawata S 2009 *Nature Photon.* **3** 473
[13] Yano T, Inouye Y and Kawata S 2006 *Nano Lett.* **6** 1269
[14] Mantooth B A, Donhauser Z J, Kelly K F and Weiss P S 2002 *Rev. Sci. Instrum.* **73** 313
[15] van Noort S J T, van der Werf K O, de Grooth B G and Greve J 1999 *Biophys. J.* **77** 2295
[16] Pohl D W and Möller R 1988 *Rev. Sci. Instrum.* **59** 840
[17] Abe M, Sugimoto Y, Custance O and Morita S 2005 *Nanotechnology* **16** 3029
[18] Mokaberi B and Requicha A 2006 *IEEE Trans. Autom. Sci. Eng.* **3** 199
[19] Proksch R and Dahlberg E D J 1993 *J. Appl. Phys.* **73** 5808
[20] Moon E E, Kupec J, Mondol M K, Smith H I and Berggren K K 2007 *J. Vac. Sci. Technol.* B **25** 2284
[21] King G M, Carter A R, Churnside A B, Eberle L S and Perkins T T 2009 *Nano Lett.* **9** 1451
[22] Denk W and Webb W W 1990 *Appl. Opt.* **29** 2382
[23] Cannara R J, Brukman M J and Carpick R W 2005 *Rev. Sci. Instrum.* **76** 053706
[24] Seitz P C, Stelzer E H K and Rohrbach A 2006 *Appl. Opt.* **45** 7309